

Temperature Effects on Donor–Acceptor Couplings in Peptides. A Combined Quantum Mechanics and Molecular Dynamics Study

Frank H. Wallrapp,[†] Alexander A. Voityuk,^{*,‡,§} and Victor Guallar^{*,†,§}

*Barcelona Supercomputing Center, Nexus II Building, 08028 Barcelona, Spain,
Institute of Computational Chemistry, University of Girona, 17071 Girona, Spain, and
Institució Catalana de Recerca i Estudis Avançats, 08010 Barcelona, Spain*

Received March 17, 2010

Abstract: We report a quantum chemistry and molecular dynamics study on the temperature dependence of electronic coupling in two short model oligopeptides. Ten nanoseconds replica exchange molecular dynamics was performed on Trp–(Pro)3–Trp and Trp–(Pro)6–Trp peptides in the gas phase in combination with computation of the energy and electronic coupling for thermal hole transfer between Trp residues. The electron transfer parameters were estimated by using the semiempirical INDO/S method together with the charge fragment difference scheme. Conformational analysis of the derived trajectories revealed that the electronic coupling becomes temperature dependent when incorporating structural dynamics of the system. We demonstrate that Trp–(Pro)3–Trp, having only few degrees of freedom, results in relatively weak couplings at low and high temperature and a strong peak at 144 K, whereas the more flexible system Trp–(Pro)6–Trp shows monotonically decreased coupling. Only a few conformations with strong donor–acceptor couplings are shown to be crucial for the overall ET rates. Our results introduce the question whether the *T* dependence of ET coupling can also be found in large biological systems.

I. Introduction

Protein-mediated long-range electron transfer (ET) between separated donor (D) and acceptor (A) sites plays a major role in biochemistry.^{1–4} It is well established that direct electron transfer is roughly exponentially dependent on the donor–acceptor distance (d_{DA}),^{5,6} whereas there is still a lively discussion on different regimes for bridge-mediated electron transfer.^{7–11} In particular, structural fluctuations of the bridge have to be taken into account^{12–14} to properly describe conformational gating mechanisms.^{15–17} Here, the ET coupling of the system depends on the thermal population of few conformational states with high coupling values.

Several studies have been published on the temperature dependence of ET rates^{18–24} and electronic conductance through molecular wires.^{25–27} Eng et al. showed that the electronic coupling between bridge-mediated donor and acceptor depends on the temperature due to the different conformations available at different temperatures.^{23,24} If donor and acceptor have a strong coupling in the energetically most favorable conformations, an increase of temperature will result in a decrease of the average coupling as the system will explore conformations with lower coupling values. On the other hand, if in the energetically most favorable conformations the couplings are weak, a temperature increase will populate conformations of higher as well as lower coupling values. Such systems are predicted to be less sensitive to temperature. Oligo *p*-phenyleneethynylene and oligofluorene bridges exemplify the first and the second regimes, respectively.²⁴ There also exists a third regime, where the most favorable conformation has a weak coupling. In this case, the average coupling will increase with the

* Corresponding author e-mail: victor.guallar@bsc.es (V.G.), alexander.voityuk@icrea.es (A.A.V.).

[†] Barcelona Supercomputing Center.

[‡] University of Girona.

[§] Institució Catalana de Recerca i Estudis Avançats.

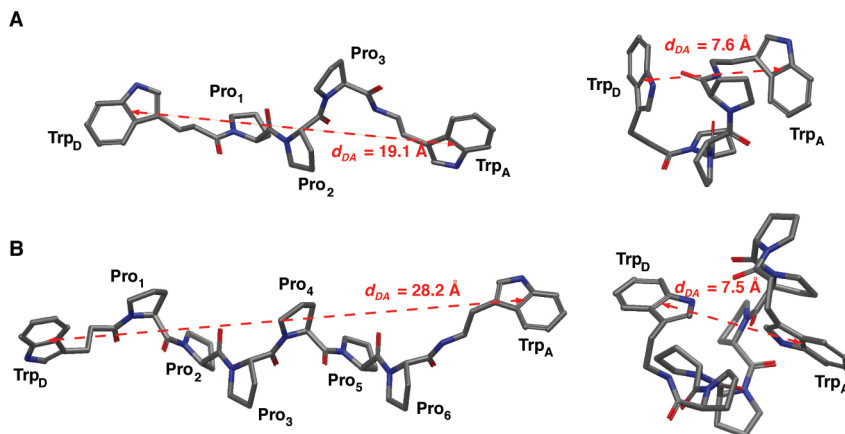


Figure 1. Oligopeptides Trp-(Pro)3-Trp and Trp-(Pro)6-Trp in panels A and B, respectively. Examples for extended and folded conformations are given for each system including their donor-acceptor distance.

temperature as demonstrated by fluorescence measurements on deoxytrinucleotides done by Jean et al.²² Additionally, there exist systems where the electronic coupling shows more complex temperature dependence, which is the case when the energy minimum does not correspond to a minimum (respectively maximum) of the electronic coupling. Examples therefore are theoretical electron transfer calculations on oligothiophene having maximal electronic coupling at about 25 K done by Eng and Albinsson²⁴ and experimental charge separation studies on 2-phenylenevinyls with a maximal rate constant at about 210 K done by Davis et al.¹⁹ In general, we can say that electronic coupling becomes temperature dependent when structural dynamics is incorporated¹⁹ and the dependence regime strongly relies on the system itself.

In prior studies, the distance dependence of electronic coupling in oligopeptides has been considered at constant temperature.^{8,10,11} In the present work, we investigate the electronic coupling for thermal hole transfer in the positively charged Trp-(Pro)3-Trp and Trp-(Pro)6-Trp oligopeptides, at a wide range of temperatures. Within the hole transfer process, where a positive charge is transferred from the donor to the acceptor, the electronic coupling can be calculated applying the one-electron or Koopmans' theorem approximation.^{28,29} Here, the properties of the adiabatic states for a radical cation can be approximated through one-electron energies and occupied molecular orbitals of the corresponding neutral (close-shell) system.³⁰ There exist several studies comparing coupling values derived from semiempirical INDO/S to those derived from ab initio calculations (including CAS-PT2 as well as CASSCF conducted on DNA bases being analogues to tryptophans) showing that the INDO/S method provides good results for electronic couplings.^{6,10,31–33} Within the presented study, we estimate coupling values using semiempirical INDO/S calculations on a set of MD trajectories obtained at different temperatures. To overcome the effect of being trapped in local minima of the energy landscape at low temperature when applying classical MD, replica-exchange molecular dynamics (REMD) was employed.³⁴ This technique exchanges conformations from different temperatures with an acceptance criteria based on the energy difference. Hence, the system can faster explore more conformational space in comparison to classical MD, when describing ensembles of conformations. The derived results

show an unexpected temperature dependence of the electronic coupling with a maximum at 144 K for Trp-(Pro)3-Trp and a monotonic decrease of the coupling for Trp-(Pro)6-Trp.

II. Methods

The oligopeptides Trp-(Pro)3-Trp and Trp-(Pro)6-Trp, shown in Figure 1, were taken from our previous work.¹⁰ We used Impact³⁵ for the REMD calculations of 10 ns in the gas phase applying NVT with the OPLS2005 force field and a nonbonded cutoff of 12 Å. We chose a temperature range of 100–502 K with 16 temperature steps determined according to Patriksson et al.³⁶ and the exchange probability of 0.4 following Denschlag et al.³⁷ Snapshots were taken every single picosecond. We excluded the data from the first nanosecond of each trajectory due to equilibration reasons as well as trajectories with temperatures higher than 413 K included for deriving better REMD sampling.

To estimate the donor-acceptor electronic coupling for hole transfer in the polypeptides, we apply the Fragment Charge Difference method (FCD).^{30,38} Like the Generalized Mulliken-Hush (GMH) method,³⁹ FCD is based on the adiabatic-to-diabatic-state transformation. Within FCD, the adiabatic states are rotated to diabatic states to maximize the charge transferred between the fragments.^{30,38} The FCD method is general and can be applied to systems containing several redox centers.^{38,40} Recently, the scheme has been extended for treatment of electronic coupling for excitation energy transfer.⁴¹ The method provides accurate results when the adiabatic states are properly defined. Comparison of GMH and FCD methods shows that in most cases both methods give very similar results.^{30,38,42} To apply the Fragment Charge Difference method, one should explicitly define D and A sites involved in ET. Therefore, there is some limitation when the method is applied to a system where donor and acceptor sites are difficult to define (e.g., a π conjugated system consisting of several aromatic rings). In our case, however, D and A are defined straightforwardly (Trp residues are considered as redox sites of interest). On the other hand, GMH can also be applied for systems where more than two non-collinear sites are involved in ET.⁴²

Within the two-state model, the bridge-mediated electronic coupling can be calculated as:

$$V_{\text{DA}} = \frac{(E_2 - E_1)|\Delta q_{12}|}{\sqrt{(\Delta q_1 - \Delta q_2)^2 + 4\Delta q_{12}^2}} \quad (1)$$

Here, Δq_1 and Δq_2 are the donor–acceptor charges difference in the two adiabatic states with their respective energies E_1 and E_2 , and Δq_{12} is the corresponding off-diagonal term. For details on computation of Δq_1 , Δq_2 , and Δq_{12} , we refer to the original publication.³⁸ Using Koopmans' theorem,⁵ we estimate the adiabatic splitting $E_2 - E_1$ through the one-electron energies of the two highest occupied molecular orbitals (HOMO and HOMO–1) calculated for the closed-shell neutral system. According to our calculation, these MOs are almost completely localized on the donor and acceptor sites. As the measurement of the coupling within each trajectory, we use its root-mean-square (rms) V_{DA} ,

$$\text{rms } V_{\text{DA}} = \sqrt{\langle V_{\text{DA}}^2 \rangle} = \sqrt{\frac{1}{n} \sum_{i=1}^n V_{\text{DA},i}^2} \quad (2)$$

where $\langle \dots \rangle$ denotes the arithmetic mean and $V_{\text{DA},i}$ denotes the electronic coupling between donor and acceptor calculated on snapshot i of all n snapshots within a single trajectory. The use of rms V_{DA} rather than $\langle V_{\text{DA}} \rangle$ is in line with the expression for the nonadiabatic CT.^{1,5} In the following, we refer to direct coupling when computing V_{DA} for systems consisting of the donor and acceptor, and the bridge-mediated coupling is calculated for systems including the donor and acceptor sites and the bridging prolines (the whole system). The ET rate was estimated using the Marcus expression:¹

$$k_{\text{ET}} = \frac{2\pi}{\hbar} V_{\text{DA}}^2 \frac{1}{\sqrt{4\pi\lambda k_{\text{B}}T}} \exp\left(-\frac{(\lambda + \Delta G^\circ)^2}{4\lambda k_{\text{B}}T}\right) \quad (3)$$

where γ is Planck's constant, k_{B} is Boltzmann's constant, λ is the reorganization energy, T is the temperature, V_{DA} is electronic coupling, and ΔG° is the Gibbs free energy change of the electron transfer reaction.

In our previous study, we demonstrated that the averaged electronic couplings derived from semiempirical INDO/S⁴³ and more sophisticated Hartree–Fock calculations are almost identical.¹⁰ Hence, we believe that the derived electronic coupling is quite reliable, although we are aware of the approximate description of the hole transfer process in the systems.

III. Results and Discussion

System Flexibility. In a preliminary study, while applying classical MD at low temperatures we were facing the problem that the system kept trapping in a low-energy conformation depending on the starting structure. The mean couplings of those trajectories were not representative, as the system did not sample its conformational space sufficiently. As a consequence, we applied REMD, which can properly sample all conformations of the system. For illustration, we plotted the rmsd of Trp–(Pro)3–Trp for both trajectories, classical MD at 125 K (in black) and REMD at 128 K (in red), calculated against their respective average conformation,

shown in Figure 2. As seen, the system gets trapped in a single low energy conformation in the case of classical MD, while REMD generates more conformations. For low temperatures, the distribution of donor–acceptor distances (Figure 3) and the mean potential energy (shown in Figure S1) are converged after 5 ns of REMD. Nevertheless, our simulations were expanded to 10 ns.

We analyze here the REMD trajectory and coupling obtained for the neutral oligopeptide. Similar results are obtained when using an MD trajectory for the positively charged peptide (results shown in the Supporting Information).

The REMD trajectories of Trp–(Pro)3–Trp reveal a complex distribution of conformations over the investigated temperature range. We measured the donor–acceptor distance d_{DA} and plotted the distribution of each trajectory as well as the mean and the standard deviation in panel A of Figure 3. Furthermore, we computed the sum of the rmsd against a folded peptide and the rmsd against a fully extended peptide for each snapshot of the REMD. From this, we calculated the standard deviation of each trajectory to get a measure of the total fluctuation of the system at a given temperature. The plot is given in panel B of Figure 3.

Oligopeptide Trp–(Pro)3–Trp generally likes to be folded at low temperature, having a short mean d_{DA} . Also, it does hardly fluctuate as seen from the small standard deviation of d_{DA} . At $T = 128$ K, it begins to explore more conformational space, reaching conformations with shorter as well as longer d_{DA} . The fluctuations increase, reaching rmsd up to 3.4 Å at $T = 161$ K. Interestingly, at $T = 128$ K the peptide has a shorter average d_{DA} than at lower temperatures, reaching more folded conformations. Starting from $T = 249$ K, Trp–(Pro)3–Trp does not change its behavior anymore and keeps the mean d_{DA} of 14.5 Å with the standard deviation of 2.8 Å. The peptide has enough heat energy to cover the large conformational space and fluctuate strongly during the MD. The total fluctuation plot, given by panel B in Figure 3, closely follows the distributions of d_{DA} . We see very low fluctuations at low temperatures, a strong increase up to $T = 161$ K, stagnation within the temperature range of $T = 201$ – 306 K, followed by a significant increase of the fluctuations at very high temperatures.

Electronic Coupling. We computed the bridge mediated as well as direct couplings between the two tryptophans in Trp–(Pro)3–Trp. The data are given in the Supporting Information and shown in Figure 4.

In general, rms V_{DA} closely follows the change of d_{DA} except in the two regions of extreme temperature (see the following paragraphs). We have high V_{DA} values for low T and low V_{DA} for high T . It shows that the low T trajectories contain more high coupling conformations in comparison to the high temperature trajectories. This comes from the fact that low energy conformations of the oligopeptide are more folded and hence have shorter d_{DA} at low T . Furthermore, the underlying regime appears to be the direct DA electronic interaction as there is no increase in the coupling when including the orbitals of the bridging prolines.

At low temperature, the coupling values of Trp–(Pro)3–Trp show unexpected behavior: rms V_{DA} increases significantly

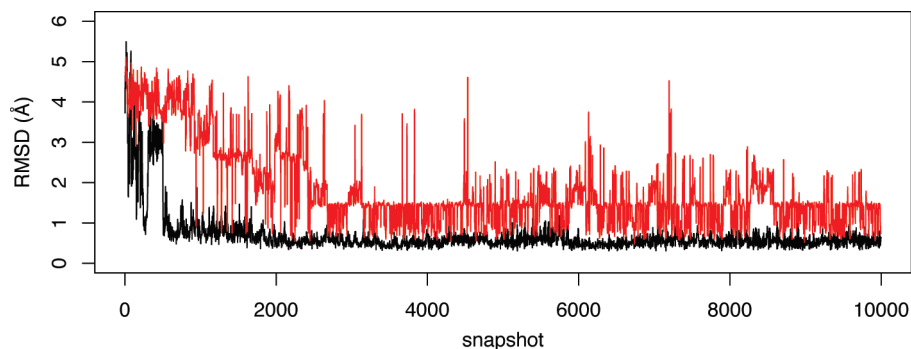


Figure 2. The rmsd of classical MD at 128 K (black) and REMD at 125 K (red) trajectories of Trp–(Pro)3–Trp.

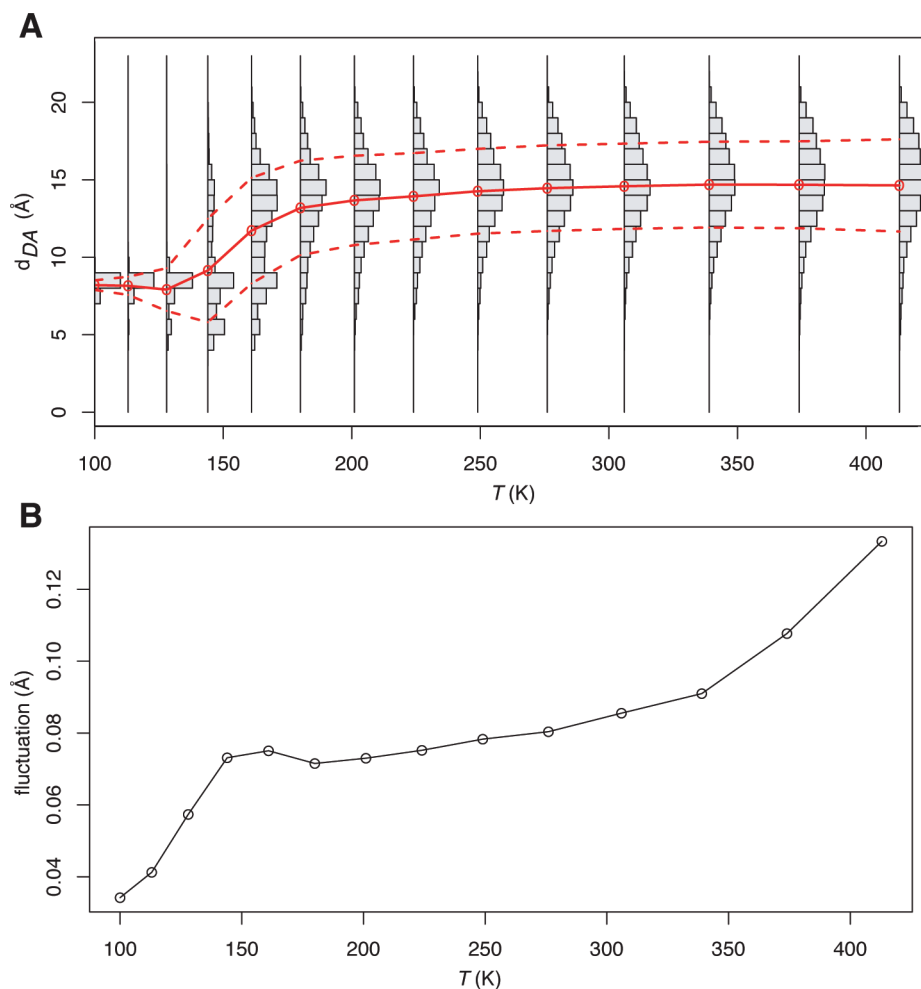


Figure 3. Panel A: Distribution of the donor–acceptor distance d_{DA} for REMD trajectories of Trp–(Pro)3–Trp. Solid and dashed red lines show the mean values and the standard deviations, respectively. Panel B: Total fluctuation of Trp–(Pro)3–Trp, given by the standard deviation within each trajectory.

from $T = 100$ to 144 K. We explain this by taking into account the fluctuation of d_{DA} at the different temperatures as shown in panel A of Figure 3. At very low temperatures (100–113 K), the peptide does not fluctuate much; the trajectories are composed of only a few conformations having very similar d_{DA} of about 8.2 Å. At slightly higher temperature (128 K), it begins to move within its limited conformational space and fluctuates only between structures of short d_{DA} . Thus, the resulting trajectories contain progressively more high-coupling conformations, increasing rms V_{DA} for $T = 128$ to 144 K. At $T = 144$ K, we see the peak of rms

V_{DA} . It matches perfectly with the distribution of d_{DA} , having higher mean d_{DA} values but, more importantly, containing also the highest fraction of short d_{DA} conformations. This discrepancy of rms V_{DA} expected from the mean conformation and actually measured rms V_{DA} can be described as conformational gating, where the electron transfer is triggered by a few strong-coupling conformations.⁴⁴

At $T > 161$ K, the peptide spends more time in extended conformations and has larger mean d_{DA} values. As a consequence, these trajectories have lower rms coupling values.

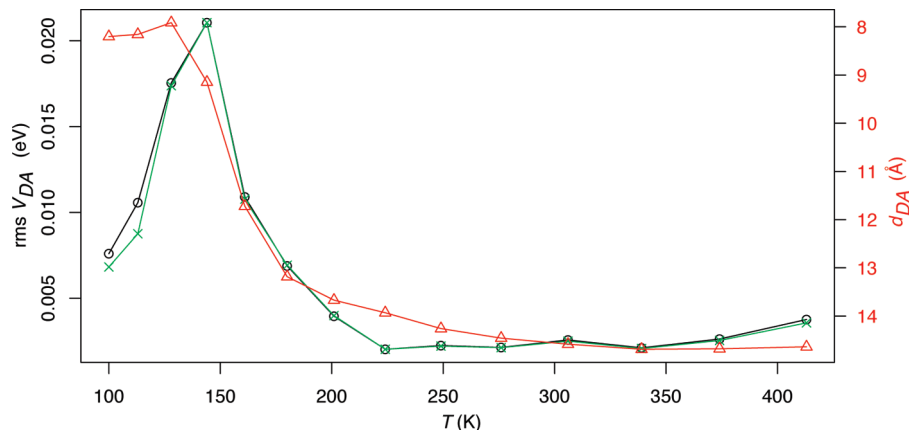


Figure 4. The rms V_{DA} plotted against temperature for Trp-(Pro)3-Trp. Color code: black, bridge-mediated coupling; green, direct coupling; and red, donor-acceptor distance d_{DA} .

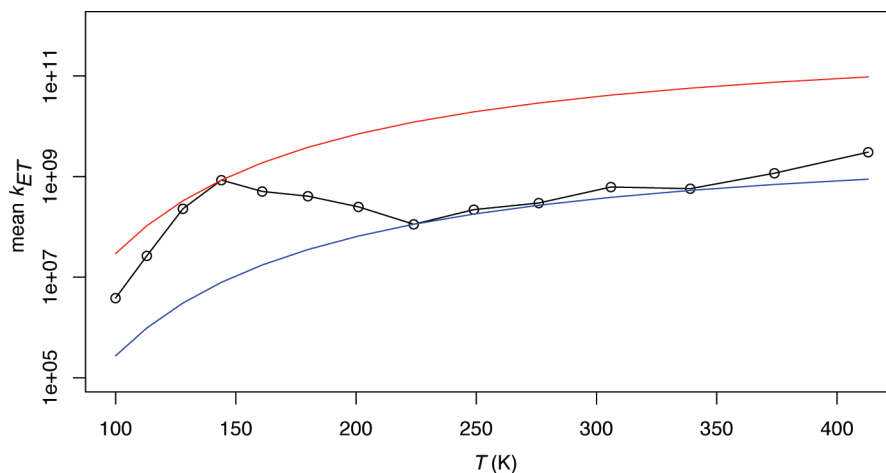


Figure 5. ET rates calculated for Trp-(Pro)3-Trp applying mean V_{DA} , $\lambda = 0.4$ eV, and $\Delta G^\circ = 0$ for each trajectory. Min k_{ET} (blue line) and max k_{ET} (red line) correspond to minimal and maximal mean values of V_{DA} .

Within the temperature range of 224–339 K, Trp-(Pro)3-Trp has enough energy to occupy nearly whole conformational space. Hence, the system contains significantly less low d_{DA} conformations when compared to the lower temperature trajectories. We see some increase of the coupling at high temperatures ranging from 376 to 413 K. This finding cannot be explained by the distance dependence of the coupling, as d_{DA} remains almost unchanged for these trajectories. For further insight, we point to the total fluctuation of the oligopeptide at these temperatures, shown in panel B of Figure 3. These high fluctuations overlay the pure d_{DA} dependence of the coupling and give the peptide the ability to acquire higher-coupling conformations, increasing the rms V_{DA} .

Rate Constants. We applied Marcus theory (eq 3) to compute the ET rate k_{ET} using the reorganization energy λ of 0.4 eV and ΔG° of zero due to identical donor and acceptor. The calculation of the reorganization energy was carried out at the B3LYP/6-31G* level. The internal reorganization energy λ_i in the gas phase was computed at the B3LYP/6-31G* level; for the Trp radical cation, the unrestricted Kohn–Sham method was applied. By definition, λ for an ET reaction is a sum of the reorganization energies of D and A. For charge transfer between identical donor and acceptor, $\lambda = 2\lambda$ (Trp). For molecule X ($X = \text{Trp}$), the

following terms were computed: (1) the energy of neutral X at the optimized geometry $E_0(X)$, (2) the energy $E_+(X^+)$ of the corresponding cation radical at the optimized geometry, (3) the energy $E_+(X)$ of neutral X calculated at the geometry of the anion radical X^+ , and (4) the energy $E_0(X^+)$ of the radical-cation state at the geometry of corresponding neutral molecule X. Thus, the reorganization energy $\lambda_i(X)$ becomes

$$\lambda = [E_+(X) - E_+(X^+) + E_0(X^+) - E_0(X)] \quad (4)$$

We estimated the mean k_{ET} by applying rms V_{DA} for each temperature trajectory of Trp-(Pro)3-Trp. Furthermore, we calculated the expected minimal and maximal rates when applying the lowest and highest coupling values, respectively. Figure 5 gives the logarithmic plot of the rates at different temperatures.

A strong increase of the rate from 100 to 144 K and then its slight decrease up to 224 K gives a peak at $T = 144$ K. At $T > 224$ K, as expected, $\log k_{ET}$ rises almost linearly with T .

Comparison between Short and Long Peptides. We also did the analysis of the temperature dependence of the coupling in the peptide having 6 proline residues instead of 3. Figure 6 shows the d_{DA} distribution, rms V_{DA} , and mean k_{ET} plots in panels A, B, and C, respectively. Trp-(Pro)6-Trp fluctuates significantly already at low temperatures (panel A). Furthermore,

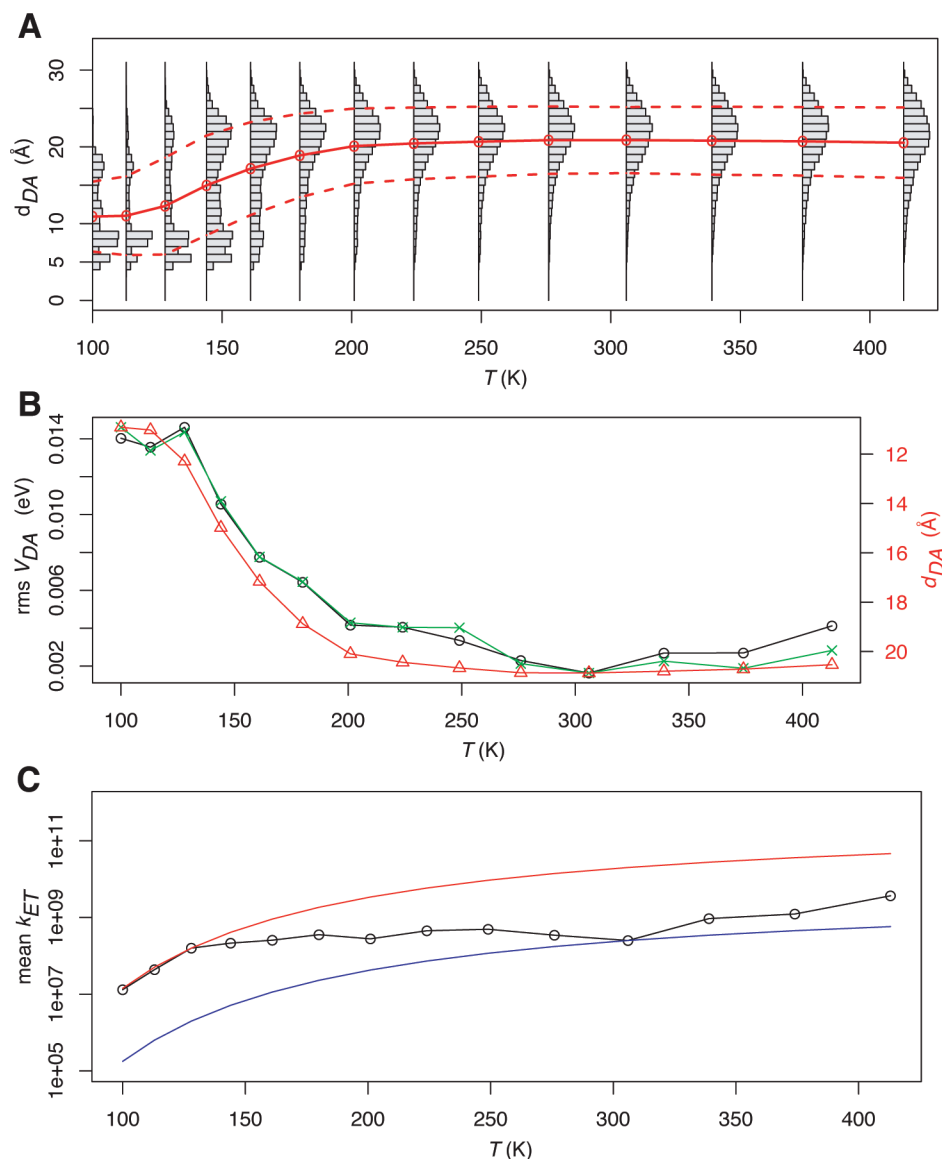


Figure 6. Results for Trp-(Pro)6-Trp. Panel A: Distribution of the donor-acceptor distance d_{DA} of each replica exchange trajectory. Solid and dashed red lines show the mean values as well as the standard deviations, respectively. Panel B: rms V_{DA} plotted against temperature. Color code: black, bridge-mediated coupling; green, direct coupling; and red, donor-acceptor distance d_{DA} . Panel C: Mean rate constant k_{ET} calculated with the rms V_{DA} , $\lambda = 0.4$ eV, and $\Delta G^\circ = 0$ for each trajectory. Min k_{ET} (blue line) and max k_{ET} (red line) correspond to minimal and maximal rms values of V_{DA} , respectively.

the system does spend most time in short d_{DA} conformations. The mean value of d_{DA} rises from about 11 Å at $T = 100$ K to about 20 Å at $T = 201$ K. At higher T , the system does not change its behavior anymore showing the normally distributed donor-acceptor distance. The rms V_{DA} as well as mean k_{ET} plots (panels B and C) show the usual temperature dependence of the coupling. We have an exponential decrease of the coupling with increasing temperature and relatively constant electron transfer rate. In trajectories higher than 300 K, we get some increase in the coupling and k_{ET} values.

We interpret the results by the following. Trp-(Pro)6-Trp has more degrees of freedom than does Trp-(Pro)3-Trp. At low temperature, each of these modes is restrained to a very little amplitude. For systems with only a few modes, these restraints prevent reaching conformations of very short d_{DA} , whereas more flexible systems are still capable of reaching low d_{DA} . As in our systems, mainly the donor-acceptor distance

gives rise to high coupling; the coupling follows closely the changes in d_{DA} , being weak for Trp-(Pro)3-Trp at very low temperature, strong around $T = 144$ K, and weak again at higher temperatures. In Trp-(Pro)6-Trp, a short d_{DA} is reached already at very low T and it increases with T , as shown in panel A of Figure 6. For completion, we also applied 10 ns REMD with a temperature range of 25–500 K on Trp-(Pro)6-Trp to study its d_{DA} at very low temperatures. The results show that Trp-(Pro)6-Trp has short d_{DA} already at 25 K. The plot of the d_{DA} distribution for $T = 25$ –418 K is given in Figure S3 of the Supporting Information.

IV. Conclusions

We have studied the temperature dependence of electronic coupling for thermal hole transfer in an oligopeptide with tryptophan-based donor and acceptor. The extensive replica

exchange molecular dynamics and conformational analysis have shown that a proper sampling at low T is very crucial in terms of electronic coupling and electron transfer rate calculations. We demonstrated that model systems with few degrees of freedom can show quite unexpected temperature-coupling dependence. For Trp-(Pro)3-Trp, there is a local peak of the rate constant at a temperature of about 144 K, whereas the more flexible peptide Trp-(Pro)6-Trp does not show such a feature. Furthermore, our results indicate that both considered oligopeptides undergo direct electron transfer as the inclusion of the bridging 3 respectively 6 prolines into the QM calculations does not increase the calculated coupling between the two tryptophans. Further characteristic therefore is the direct dependence of V_{DA} to d_{DA} of the applied oligopeptides as extensively discussed on our previous work.¹⁰

Previously, we showed for these model systems that solvent can influence the electronic coupling due to restriction of the thermally accessible conformational space.¹⁰ This may modulate the system behavior, reducing the effects discussed above. Nevertheless, our results raise the question of whether the temperature dependence similar to that we found for Trp-(Pro)3-Trp would also exist in biological systems where the protein matrix essentially affects the overall conformational dynamics.

Acknowledgment. This work was supported by a grant from the Spanish Ministry of Education and Science to V.G. through the project CTQ200762122 as well as to A.A.V. through the project CTQ2009-12346. Computational resources were provided by Barcelona Supercomputing Center and University of Girona.

Supporting Information Available: A plot of the average potential energy against the temperature for each trajectory of the REMD for Trp-(Pro)3-Trp, a plot of the d_{DA} distribution and the electronic coupling of the REMD on cationic Trp-(Pro)3-Trp, and the d_{DA} distribution for the REMD on Trp-(Pro)6-Trp with temperatures ranging from 25 to 500 K. Furthermore, two tables listing the mean d_{DA} , rms V_{DA} , and their fluctuations derived for both Trp-(Pro)3-Trp and Trp-(Pro)6-Trp. This material is available free of charge via the Internet at <http://pubs.acs.org>.

References

- Marcus, R. A.; Sutin, N. *Biochim. Biophys. Acta* **1985**, *811*, 265–322.
- Beratan, D. N.; Onuchic, J. N.; Winkler, J. R.; Gray, H. B. *Science* **1992**, *258*, 1740–1741.
- Gray, H. B.; Winkler, J. R. *Annu. Rev. Biochem.* **1996**, *65*, 537–561.
- Balzani, V.; Piotrowiak, P.; Rodgers, M. A. J.; Mattay, J.; Astruc, D.; Gray, H. B.; Fukuzumi, S.; Mallouk, T. E.; Haas, Y.; de Silva, A. P.; Gould, I. R. *Electron Transfer in Chemistry*; Wiley-VCH: Weinheim, Germany, 2001; Vols. I–V.
- Newton, M. D. *Chem. Rev.* **1991**, *91*, 767–792.
- Ungar, L. W.; Newton, M. D.; Voth, G. A. *J. Phys. Chem. B* **1999**, *103*, 7367–7382.
- Isied, S. S.; Ogawa, M. Y.; Wishart, J. F. *Chem. Rev.* **1992**, *92*, 381–394.
- Ogawa, M. Y.; Wishart, J. F.; Young, Z.; Miller, J. R.; Isied, S. S. *J. Phys. Chem.* **1993**, *97*, 11456–11463.
- Felts, A. K.; Pollard, W. T.; Friesner, R. A. *J. Phys. Chem.* **1995**, *99*, 2929–2940.
- Wallrapp, F.; Voityuk, A.; Guallar, V. *J. Chem. Theory Comput.* **2009**, *5*, 3312–3320.
- Malak, R. A.; Gao, Z.; Wishart, J. F.; Isied, S. S. *J. Am. Chem. Soc.* **2004**, *126*, 13888–13889.
- Kawatsu, T.; Kakitani, T.; Yamato, T. *J. Phys. Chem. B* **2002**, *106*, 11356–11366.
- Skourtis, S. S.; Balabin, I. A.; Kawatsu, T.; Beratan, D. N. *Proc. Natl. Acad. Sci. U.S.A.* **2005**, *102*, 3552–3557.
- Balabin, I. A.; Beratan, D. N.; Skourtis, S. S. *Phys. Rev. Lett.* **2008**, *101*, 158102–158104.
- Hoffman, B. M.; Ratner, M. A. *J. Am. Chem. Soc.* **1987**, *109*, 6237–6243.
- Balabin, I. A.; Onuchic, J. *Science* **2000**, *290*, 114–117.
- Hartings, M. R.; Kurnikov, I. V.; Dunn, A. R.; Winkler, J. R.; Gray, H. B.; Ratner, M. A. *Coord. Chem. Rev.* **2010**, *254*, 248–253.
- Read, I.; Napper, A.; Kaplan, R.; Zimmt, M. B.; Waldeck, D. H. *J. Am. Chem. Soc.* **1999**, *121*, 10976–10986.
- Davis, W. B.; Ratner, M. A.; Wasielewski, M. R. *J. Am. Chem. Soc.* **2001**, *123*, 7877–7886.
- Huppman, P.; Arlt, T.; Penzkofer, H.; Schmidt, S.; Bibikova, M.; Dohse, B.; Oesterhelt, D.; Wachtveit, J.; Zinth, W. *Biophys. J.* **2002**, *82*, 3186–3197.
- Napper, A. M.; Read, I.; Waldeck, D. H.; Kaplan, R. W.; Zimmt, M. B. *J. Phys. Chem. A* **2002**, *106*, 4784–4793.
- Jean, J. M.; Krueger, B. P. *J. Phys. Chem. B* **2006**, *110*, 2899–2909.
- Eng, M. P.; Martensson, J.; Albinsson, B. *Chem.-Eur. J.* **2008**, *14*, 2819–2826.
- Eng, M. P.; Albinsson, B. *Chem. Phys.* **2009**, *357*, 132–139.
- Selzer, Y.; Cabassi, M. A.; Mayer, T. S.; Allara, D. L. *J. Am. Chem. Soc.* **2004**, *126*, 4052–4053.
- Poot, M.; Osorio, E.; O'Neill, K.; Thijssen, J. M.; Vanmaekelbergh, D.; van Walree, C. A.; Jenneskens, L. W.; van der Zant, H. S. J. *Nano Lett.* **2006**, *6*, 1031–1035.
- Haiss, W.; Zalinge, H. v.; Bethell, D.; Ulstrup, J.; Schiffrin, D. J.; Nichols, R. J. *Faraday Discuss.* **2006**, *131*, 253–264.
- Liang, C.; Newton, M. D. *J. Phys. Chem.* **1992**, *96*, 2855–2866.
- Onuchic, J. N.; Beratan, D. N.; Hopfield, J. J. *J. Phys. Chem.* **1986**, *90*, 3707–3721.
- Rösch, N.; Voityuk, A. A. Quantum Chemical Calculation of Donor-Acceptor Coupling for Charge Transfer in DNA. *Long-Range Charge Transfer in DNA II*; 2004; pp 37–72.
- Prytkova, T. R.; Kurnikov, I. V.; Beratan, D. N. *J. Phys. Chem. B* **2005**, *109*, 1618–1625.
- Lambert, C.; Amthor, S.; Schelter, J. J. *J. Phys. Chem. A* **2004**, *108*, 6474–6486.
- Voityuk, A. *Chem. Phys. Lett.* **2006**, *427*, 177–180.

- (34) Sugita, Y.; Okamoto, Y. *Chem. Phys. Lett.* **1999**, *314*, 141–151.
- (35) *Impact*, 5.0 ed.; Schrödinger, LCC: New York, NY, 2008.
- (36) Patriksson, A.; Spoel, D. v. d. *Phys. Chem. Chem. Phys.* **2008**, *10*, 2073–2077.
- (37) Denschlag, R.; Lingenheil, M.; Tavan, P. *Chem. Phys. Lett.* **2009**, *473*, 193–195.
- (38) Voityuk, A. A.; Rosch, N. *J. Chem. Phys.* **2002**, *117*, 5607–5616.
- (39) Cave, R. J.; Newton, M. D. *J. Chem. Phys.* **1997**, *106*, 9213–9226.
- (40) Voityuk, A. A. *J. Phys. Chem. B* **2005**, *109*, 17917–17921.
- (41) Hsu, C.-P.; You, Z.-Q.; Chen, H.-C. *J. Phys. Chem. C* **2008**, *112*, 1204–1212.
- (42) Subotnik, J. E.; Cave, R. J.; Steele, R. P.; Shenvi, N. *J. Chem. Phys.* **2009**, *130*, 234102–234102.
- (43) Ridley, J.; Zerner, M. *Theor. Chem. Acc.* **1973**, *32*, 111–134.
- (44) Berlin, Y. A.; Burin, A. L.; Siebbeles, L. D. A.; Ratner, M. A. *J. Phys. Chem. A* **2001**, *105*, 5666–5678.

CT100363E